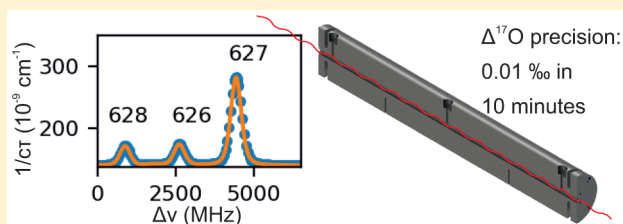


Direct, Precise Measurements of Isotopologue Abundance Ratios in CO₂ Using Molecular Absorption Spectroscopy: Application to $\Delta^{17}\text{O}$ Tim Stoltmann,^{†,‡,§} Mathieu Casado,[§] Mathieu Daëron,[§] Amaelle Landais,[§] and Samir Kassi^{*,†,‡}[†]CNRS, LIPhy, F-38000 Grenoble, France[‡]Université Grenoble Alpes, LIPhy, F-38000 Grenoble, France[§]Laboratoire des Sciences du Climat et de l'Environnement, LSCE/IPSL, CEA-CNRS-UVSQ, Université Paris-Saclay, F-91191 Gif-sur-Yvette, France

ABSTRACT: We present an ultrasensitive absorption spectrometer based on a 30 Hz/s stability, sub-kHz line width laser source coupled to a high-stability cavity-ring-down-spectroscopy setup. It provides direct and precise measurements of the isotopic ratios $\delta^{17}\text{O}$ and $\delta^{18}\text{O}$ in CO₂. We demonstrate the first optical absorption measurements of ¹⁷O anomalies in CO₂ with a precision better than 10 ppm, matching the requirements for paleo-environmental applications. This illustrates how optical absorption methods have become a competitive alternative to state-of-the-art isotopic ratio mass spectrometry techniques.



Non-mass-dependent stable isotopic anomalies are deviations from an assumed mass-dependent fractionation law (e.g., Young et al.¹). ¹⁷O anomalies can be observed in a variety of environments, associated with different processes. Commonly, ¹⁷O anomalies are expressed in the $\Delta^{17}\text{O}$ notation. In this study, we use a logarithmic expression,^{1,18,19} where λ_R denotes the slope of a reference line R:

$$\Delta^{17}\text{O} = \ln(\delta^{17}\text{O} + 1) - \lambda_R \times \ln(\delta^{18}\text{O} + 1)$$

Several values for λ_R have been reported, each adapted for or coming from different environmental systems. In this study, we have chosen a value of 0.528. $\delta^{17}\text{O}$ and $\delta^{18}\text{O}$ are referenced to arbitrary fixed values for now, as we solely intend to prove the instrumental precision of our prototype. $\Delta^{17}\text{O}$ of CO₂ has been proposed to be used as a proxy for terrestrial gross carbon fluxes^{2,3} or marker for deep stratospheric intrusions.^{4,17} ¹⁷O anomaly in water bodies are an established tracer for evaporation processes,^{5,6} which has been used extensively in geoscientific studies. The ¹⁷O-anomaly of carbonate rocks, in turn, reflects the anomaly of the respective parent water, thus constituting a valuable tracer for paleo-hydrologic processes. High-resolution terrestrial archives such as speleothems or limnic carbonates therefore could give extensive insight into past moisture sources and/or atmospheric convection regimes.

The determination of $\Delta^{17}\text{O}$ in CO₂ requires precise measurements of three isotopologues: ¹⁶O¹²C¹⁶O, ¹⁶O¹²C¹⁸O, and ¹⁶O¹³C¹⁷O. Typically, the required precision levels call for the use of state of the art isotopic ratio mass spectrometry (IRMS) techniques. However, because of isobaric interferences of ¹⁶O¹³C¹⁶O (1.1%) and ¹⁶O¹²C¹⁷O (0.076%), ¹⁷O measurements in CO₂ have so far remained highly challenging. Several methods have been developed in previous years, mainly based on IRMS methods following oxygen exchanges through

fluorination,⁷ exchange with solid (cerium or copper) oxide,^{8–10} CO₂–water equilibration.^{3,11} An analytical challenge is also to be able to measure this anomaly in small stratospheric samples (e.g., Mrozek et al.¹²). The best precision reported until now is 10, 30, and 5 ppm for $\delta^{17}\text{O}$, $\delta^{18}\text{O}$, and $\Delta^{17}\text{O}$ of CO₂,¹¹ respectively (1000 ppm = 1 ‰). Those methods come at a significant cost of time and resources.

Spectroscopic methods offer an appealing alternative in this field, since they probe absorption frequencies unambiguously associated with the internal distribution of mass rather than the total mass of an isotopologue, so they are unaffected by isobaric interferences. The precise spectroscopic determination of isotopologue ratios, however, requires an accurate and precise determination of absorption line shapes.

Only few approaches toward high precision measurements of $\delta^{17}\text{O}$ in CO₂ have been made.^{13,14} The highest precision reported to date is 590 ppm, by Long et al. in 2011.¹⁴ Note that a spectrometer with infinite signal-to-noise on the y axis would finally be limited by the conversion of laser frequency noise to amplitude noise as it probes absorption line wings. Our work builds on previous work by Burkart et al.,¹⁵ which offers exceptional laser frequency stability by using a new kind of laser source obtained by optical feedback locking of a distributed feedback laser (DFB) to an ultrastable V-shaped optical cavity. We describe several improvements to the original setup and report on the performance levels of a prototype with a relative frequency-stability better than 2×10^{-12} and an absorption detection limit of $5 \times 10^{-13} \text{ cm}^{-1}$, allowing for high-precision determination of isotopic ratios.

Received: July 20, 2017

Accepted: September 11, 2017

Published: September 11, 2017

EXPERIMENTAL SETUP

The experimental setup comprises of a very narrow and stable V-shaped optical feedback source (VCOF)¹⁵ lasing in the near-infrared around 1.6 μm , which provides a sub-kHz laser line width with a typical drift of 30 Hz/s. Locking of a distributed feedback diode laser to the cavity is realized by a mirror mounted on a piezo-electric actuator (PZT1), which is controlled by a lock-in-amplifier regulating on the transmission signal of VCOF. 80% of the emitted light is collimated (L1) in an optical fiber. To allow continuous frequency tuning over a 19 GHz range, a fibered multiple Mach-Zehnder modulator (MZM, Photline MXIQ-LN40), used as an optical Single-Sideband generator (SSB),¹⁵ is modulated by a radio frequency. This solution allows arbitrary distribution of spectral points on the frequency axis and therefore focusing on regions of importance for line shape definition, to increase measurement precision. The frequency shifted light is amplified by a boost optical amplifier (BOA) and can be interrupted by an acousto-optic-modulator (AOM). Finally, a second collimator (L2) allows free-space coupling to a high-sensitivity, high-stability cavity ring down spectrometer (CRDS) setup. The CRDS cavity is made of a massive aluminum rod (70 mm outer diameter, 8 mm inner diameter, 490 mm length) fitted with two high reflectivity mirrors (Layertec GmbH). The optical resonator exhibits a finesse of 450 000 with an FSR of 297 MHz. The rear mirror is mounted on a piezo-electric tube actuator (PZT, Physikinstrumente P-016.10H) to allow for length dithering of the cavity. The alignment of the cavity is realized by acting on 8-push- and 8 pull-screws. Two external mirrors mounted on piezo-electric-actuators (PZT2, PZT3) allow to average out effects of spurious reflections on optics elements. The reader will find a detailed description of the technique in Burkart et al.²³ The whole CRDS setup is mounted in a temperature stabilized enclosure, and the cavity itself is further stabilized at a level of a few mK. The cavity temperature is recorded by two PT1000 elements embedded in the aluminum body.

CRDS Stability. A major difference to the setup proposed by Burkart et al.¹⁶ is the simplification of the optical resonator-optical source locking scheme, by abandoning a complex Pound-Drever-Hall locked system and switch for a simpler weak-locked system, satisfactory for isotopic ratio measurements. It results in a more robust and faster system at the price of a negligibly imperfect optical phase transfer resulting in higher demands in system stability. Active temperature stabilization of the CRDS cavity is realized by a homemade, stand-alone, PID system based on an Arduino Due micro-controller. The PID receives temperature readings from one of the PT1000 probes embedded in the aluminum body, close to the analyte gas, and acts on a resistive heating band (OMEGA SRFG-XXX/10-P). To minimize environmental influence, the whole CRDS-setup is mounted inside an insulating wooden enclosure. This limits temperature gradients in the gas cell to less than 10 mK. Pressure stabilization for flow measurements is done by a (Bürkert 2/2) proportional valve, acting on readings from a (MKS Baratron 626B, 100 Torr) capacitive gauge. Control of the electro valve is done by homemade control electronics working with a LabVIEW VI. Using this system, we reach a precision of the pressure regulation of 0.2 μbar .

Comb Referencing. The VCOF used in the current setup shows a typical drift of 30 Hz/s and long-term oscillations with a peak-to-peak excursion of about 6 MHz, mainly due to the

composite character of the cavity, involving low-expansion glass and INVAR flanges for the mirror mounts. To overcome the limitations imposed by this frequency instability, our VCOF is referenced to a GPS-referenced femtosecond comb^{20,21} with a repetition rate of 250 MHz. In total, 5 % of the available laser light are used to set up a beat-note with the comb. A fast Fourier transform of the beat note signal provides us with the distance in frequency space between our laser source and the closest comb tooth. A Fizeau type wavemeter (HighFinesse WS-UIR) with a precision of 10 MHz allows for determination of the respective comb tooth used for referencing. This referencing of our laser source allows for instantaneous correction of the observed drift. This level of frequency stability allows an optimal retrieval of line surfaces and thus gives the long-term stability needed for spectral averaging.

Locking System. The cavity length is weak-locked to the laser frequency. The lock is reached and maintained by a homemade system comprising of three principal components. A piezo-electric tube actuator (PZT, see Figure 1) is dithering

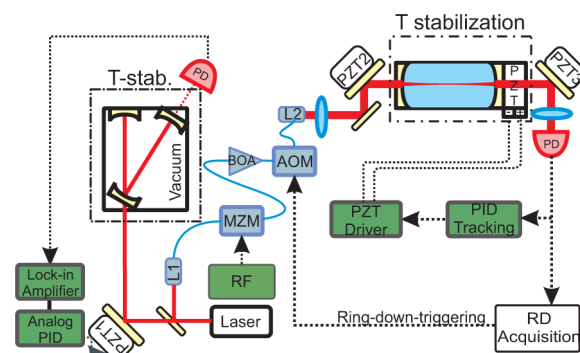


Figure 1. Experimental setup of a VCOF-CRDS system. On the left-hand side is a v-shaped, evacuated cavity in a thermalized enclosure. On the right side is a CRDS-setup in a thermalized enclosure.

the length of the optical resonator on the pm scale. The PZT is driven by an ultralow noise (PD μ 150, PiezoDrive) piezo driver over a range of 100 V. Control is realized by an analog PID board triggered by the photodiode output. A constant, symmetric, 100 Hz triangle modulation with an amplitude of 0.2 V is added on the PZT. The modulation amounts to an effective length dithering of the cavity of about 0.3% of the FSR, allowing the generation of passages through resonance. A signed error signal is derived from the sign and amplitude of the modulation voltage at the moment the passage through resonance occurs.

The error signal is sent to a PID that keeps the modulation centered over extended periods of time. The relocking time of this system is on the order of 2 s. Once locked, the system reaches a typical repetition rate of 200 ring-downs per second.

Acquisition and Spectral Treatment. In order to exclude potential effects of gas exchange or adsorption on the cell walls, measurements are currently performed using a stable flow of pure CO_2 at 20 mbar. The flow rate is 0.6 mL/min which corresponds to 25 $\mu\text{mol}/\text{min}$. The fully automatic spectral acquisition follows an interlacing scheme to minimize time losses. In this scheme, the cavity is locked to the laser frequency and the MZM is used to jump over multiples of the CRDS FSR subsequently. To increase the resolution this pattern is shifted. This restricts the necessary relocking of the cavity to the laser

frequency to a minimum, when the pattern is shifted, making the amount of relocks a function of the spectral resolution.

Additionally, because our setup is able to arbitrarily place spectral points, we constrained the top of absorption peaks by increasing the spectral density. This results in an average acquisition time of 47 s per spectrum, dominated by the fact that adding constraining points on the peak implies a series of additional relocks. Part of the lost time is due to a diminished repetition rate at strong absorptions, which can be optimized by using an adaptive system. The data is then fitted using the Minit2 (CERN) function minimizing tool to retrieve absorption line surfaces, which gives the base for the described ratio calculations. The line shape of the absorption profile is fitted using a speed-dependent-Nelkin-Ghatak profile (SDNGP¹⁷). It has been shown in previous studies, that SDNGP is well suited to account for collisional narrowing and speed dependent collisional broadening effects in the present pressure regime¹⁴ in order to increase the accuracy of ratio determination. The pressure broadening coefficients are provided by the HITRAN2012 database and scaled according to the gas pressure. The Doppler width is fixed according to molecular mass and cell temperature. The other parameters, proportional to pressure, have been determined experimentally. Only the line amplitude is kept free. Using this procedure, we reach a standard deviation of the fit of $4.2 \times 10^{-12} \text{ cm}^{-1}$, see Figure 2. Since the precision of the retrieved line profiles from

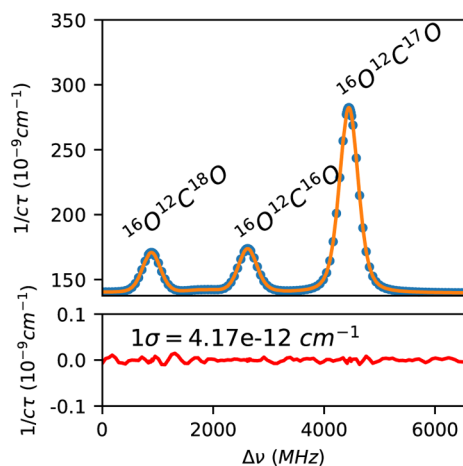


Figure 2. Typical absorption spectrum and the corresponding fit and fit residuals. Frequency is given as detuning from 188,421,366 MHz. The standard deviation of the fit is $4.2 \times 10^{-12} \text{ cm}^{-1}$.

one single spectrum is not sufficient for the subtle changes that need to be resolved, we average the values from several subsequent spectra.

EXPERIMENTAL PERFORMANCE

Figure 3 shows the instrumental precision of our instrument in terms of an Allan-standard deviation plot (using an overlapping Allan-Variance for increased statistical confidence) for a $\Delta^{17}\text{O}$ measurement series.

Figure 3 shows the evolution of the measurement precision over averaging time. The green trace shows the simulation of an ideal, unbiased, and purely statistical behavior. In blue we show untreated $\Delta^{17}\text{O}$ values from a typical measurement series, with the points marking individual spectra. Exhibiting an initial precision of 31.5 ppm, the maximum precision is reached after 16 min with a precision of 10.3 ppm. From there onward the

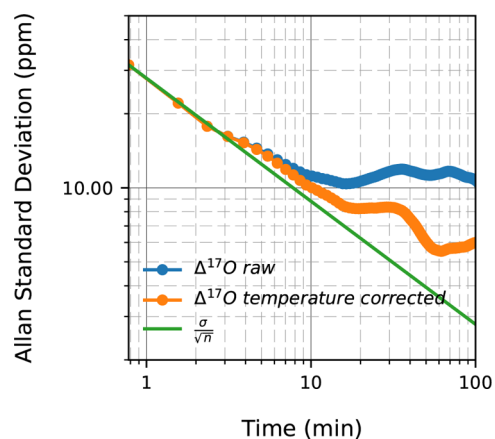


Figure 3. Allan standard deviation of a typical $\Delta^{17}\text{O}$ measurement series. Denoted in blue, the uncorrected data set. Denoted in orange, the same data set with a temperature gradient correction applied.

precision oscillates marking an underlying bias which prohibits further averaging of measurement values but also showing a stability at a level significantly below 15 ppm. Figure 4 shows the raw $\Delta^{17}\text{O}$ values and the temperature gradient.

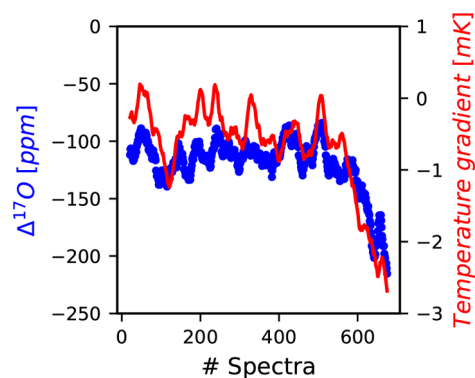


Figure 4. In blue, the raw $\Delta^{17}\text{O}$ values used in this study. The red curve shows the temperature gradient measured on the CRD-cell. Both curves show the rolling mean over 15 samples of the raw data. A clear correlation of both parameters becomes obvious. Note that the gradient is retrieved within two drillings inside the massive aluminum body. While this allows correcting for biases caused by temperature changes in the gas, it will be less suitable for corrections of biases introduced by affected pressure gauges or valves.

A correlation of the two parameters is observed. A direct correction using the correlation factor between ratio and gradient would, however, not be sufficient, since from a physical point of view the three absorption lines involved exhibit different temperature sensitivities. The retrieved line surfaces are thus affected to a different extent. We therefore implemented a temperature correction of the retrieved line surfaces based on T-dependencies retrieved from the HITRAN²² database. The orange curve in Figure 3 shows the Allan-Variance of the same data set after temperature correction. An improvement of the data quality is clearly visible, with the instrumental precision reaching 10 ppm after 10 min of measurement time. The Allan SD finally starts oscillating between 5.5 and 9 ppm, which is likely due to very small temperature effects that we do not yet sufficiently account for.

CONCLUSION

We developed a new instrument for the direct measurement of $\Delta^{17}\text{O}$ in CO_2 . This instrument is based on optical feedback frequency stabilized cavity ring down spectroscopy near $1.6\ \mu\text{m}$ ¹⁶ and incorporates an ultrastable and ultranarrow laser source, coupled with a high stability CRDS setup. We demonstrated an instrumental precision of better than 10 ppm within 10 min of measurement time, requiring 300 μmol of pure CO_2 . The predominant current limitations arise from the temperature sensitivity of absorption lines. However, we identified alternative absorption lines of a comparable signal/noise ratio with a reduced temperature sensitivity and envision using those together with an improved cell temperature management to limit the need for temperature corrections in routine measurements. To our best knowledge, this is currently the fastest method for such measurements and the way to quick and direct routine measurements of $\Delta^{17}\text{O}$ in CO_2 .

AUTHOR INFORMATION

Corresponding Author

*E-mail: samir.kassi@univ-grenoble-alpes.fr.

ORCID

Tim Stoltmann: 0000-0002-3047-128X

Notes

The authors declare no competing financial interest.

ACKNOWLEDGMENTS

This work was supported by the Agence Nationale de la Recherche (Grant ANR-13-JS060005), Institut National des Sciences de l'Univers (LEFE/CHAT) and Labex OSUG@2020 (Grant ANR10 LABX56). We are grateful to the Université Joseph Fourier and the GRAM Equipex REFIMEVE+ for additional financial support. M.C and A.L have received funding from the European Research Council under the European Union's Seventh Framework Programme (Grant FP7/2007-2013)/RC Grant Agreement Number 306045. The authors also want to thank Alain Campargue and Erik Kerstel for fruitful discussions. The authors thank two anonymous reviewers whose comments improved the quality of this article.

REFERENCES

- (1) Young, E. D.; Galy, A.; Nagahara, H. *Geochim. Cosmochim. Acta* **2002**, *66*, 1095–1104.
- (2) Boering, K.; Jackson, T.; Hoag, K.; Cole, A.; Perri, M.; Thiemens, M.; Atlas, E. *Geophys. Res. Lett.* **2004**, *31*, 31.
- (3) Hofmann, M.; Horváth, B.; Schneider, L.; Peters, W.; Schützenmeister, K.; Pack, A. *Geochim. Cosmochim. Acta* **2017**, *199*, 143–163.
- (4) Liang, M.-C.; Mahata, S. *Sci. Rep.* **2015**, *5*, 11352.
- (5) Winkler, R.; Landais, A.; Sodemann, H.; Dümbgen, L.; Prié, F.; Masson-Delmotte, V.; Stenni, B.; Jouzel, J. *Clim. Past* **2012**, *8*, 1–16.
- (6) Uemura, R.; Barkan, E.; Abe, O.; Luz, B. *Geophys. Res. Lett.* **2010**, *37*, L04402.
- (7) Bhattacharya, S.; Thiemens, M. *Z. Naturforsch., A: Phys. Sci.* **1989**, *44*, 435–444.
- (8) Assonov, S.; Brenninkmeijer, C. *Rapid Commun. Mass Spectrom.* **2001**, *15*, 2426–2437.
- (9) Kawagucci, S.; Tsunogai, U.; Kudo, S.; Nakagawa, F.; Honda, H.; Aoki, S.; Nakazawa, T.; Gamo, T. *Anal. Chem.* **2005**, *77*, 4509–4514.
- (10) Hofmann, M. E.; Pack, A. *Anal. Chem.* **2010**, *82*, 4357–4361.
- (11) Barkan, E.; Luz, B. *Rapid Commun. Mass Spectrom.* **2012**, *26*, 2733–2738.

- (12) Mrozek, D. J.; van der Veen, C.; Hofmann, M. E.; Chen, H.; Kivi, R.; Heikkinen, P.; Röckmann, T. *Atmos. Meas. Tech.* **2016**, *9*, 5607.
- (13) Castrillo, A.; Casa, G.; Gianfrani, L. *Opt. Lett.* **2007**, *32*, 3047–3049.
- (14) Long, D.; Okumura, M.; Miller, C.; Hodges, J. *Appl. Phys. B: Lasers Opt.* **2011**, *105*, 471–477.
- (15) Burkart, J.; Romanini, D.; Kassi, S. *Opt. Lett.* **2013**, *38*, 2062–2064.
- (16) Burkart, J.; Romanini, D.; Kassi, S. *Opt. Lett.* **2014**, *39*, 4695–4698.
- (17) Long, D. A.; Bielska, K.; Lisak, D.; Havey, D. K.; Okumura, M.; Miller, C. E.; Hodges, J. T. *J. Chem. Phys.* **2011**, *135*, 064308.
- (18) Hulston, J.; Thode, H. *J. Geophys. Res.* **1965**, *70*, 3475–3484.
- (19) Miller, M. F. *Geochim. Cosmochim. Acta* **2002**, *66*, 1881–1889.
- (20) Stone, J. A.; Egan, P. *J. Res. Natl. Inst. Stand. Technol.* **2010**, *115*, 413–431.
- (21) Burkart, J.; Sala, T.; Romanini, D.; Marangoni, M.; Campargue, A.; Kassi, S. *J. Chem. Phys.* **2015**, *142*, 191103.
- (22) Rothman, L. S.; Gordon, I. E.; Babikov, Y.; Barbe, A.; Benner, D. C.; Bernath, P. F.; Birk, M.; Bizzochi, L.; Boudon, V.; Brown, L. R.; et al. *J. Quant. Spectrosc. Radiat. Transfer* **2013**, *130*, 4–50.
- (23) Burkart, J.; Kassi, S. *Appl. Phys. B: Lasers Opt.* **2015**, *119*, 97–109.